

BRIEF REPORT

 OPEN ACCESS

## Tertiary lymphoid structures are confined to patients presenting with unifocal Langerhans Cell Histiocytosis

Willemijn T. Quispel<sup>a</sup>, Eline C. Steenwijk<sup>a</sup>, Vincent van Unen<sup>a</sup>, Susy J. Santos<sup>a</sup>, Lianne Koens<sup>b</sup>, Reina Mebius<sup>c</sup>, R. Maarten Egeler<sup>d,\*</sup>, and Astrid G. S. van Halteren<sup>a,\*</sup>

<sup>a</sup>Immunology Laboratory, Willem Alexander Children's Hospital, Leiden University Medical Center, Leiden, the Netherlands; <sup>b</sup>Department of Pathology, Leiden University Medical Center, Leiden, the Netherlands; <sup>c</sup>Department of Molecular Cell Biology and Immunology, VU University Medical Center, Amsterdam, the Netherlands; <sup>d</sup>Division of Hematology/Oncology, University of Toronto/Hospital for Sick Children, Toronto, Canada

### ABSTRACT

Langerhans cell histiocytosis (LCH) is a neoplastic myeloid disorder with a thus far poorly understood immune component. Tertiary lymphoid structures (TLS) are lymph node-like entities which create an immune-promoting microenvironment at tumor sites. We analyzed the presence and clinical relevance of TLS in  $n = 104$  H&E-stained, therapy-naïve LCH lesions of non-lymphoid origin and applied immunohistochemistry to a smaller series. Lymphoid-follicular aggregates were detected in 34/104 (33%) lesions. In line with the lymphocyte recruitment capacity of MECA-79<sup>+</sup> high endothelial venules (HEVs), MECA-79<sup>+</sup>-expressing-LCH lesions (37/77, 48%) contained the most CD3<sup>+</sup> T-lymphocytes ( $p = 0.003$ ). TLS were identified in 8/15 lesions and contained T- and B-lymphocytes, Follicular Dendritic Cells (FDC), HEVs and the chemokines CXCL13 and CCL21 representing key cellular components and TLS-inducing factors in conventional lymph nodes (LN). Lymphoid-follicular aggregates were most frequently detected in patients presenting with unifocal LCH (24/70, 34%) as compared to patients with poly-ostotic or multi-system LCH (7/30, 23%,  $p = 0.03$ ). In addition, patients with lymphoid-follicular aggregates-containing lesions had the lowest risk to develop new LCH lesions ( $p = 0.04$ ). The identification of various stages of TLS formation within LCH lesions may indicate a key role for the immune system in controlling aberrant histiocytes which arise in peripheral tissues.

**Abbreviations:** FDC, Follicular Dendritic Cells; FFPE, Formalin-fixed paraffin-embedded; H&E, Hematoxylin/Eosin; HEVs, High Endothelial Venules; LCH, Langerhans Cell Histiocytosis; LN, Lymph nodes; PNAd, Peripheral lymph Node Addressins; T-reg, Regulatory T-cells; TLS, Tertiary lymphoid structures

### ARTICLE HISTORY

Received 18 December 2015  
Revised 4 March 2016  
Accepted 5 March 2016

### KEYWORDS

High endothelial venules; inflammatory; Langerhans cell histiocytosis; lymphocytes; lymphoid aggregates; myeloid neoplastic; prognosis; tertiary lymphoid structures

### Introduction

Chronically inflamed and cancerous non-lymphoid tissues often contain organized lymphocyte aggregates called TLS.<sup>1,2</sup> TLS closely resemble normal lymph nodes with regard to cellular composition and structural organization, chemokine expression and specialized microvasculature such as HEVs.<sup>3</sup> HEVs have been detected, among others, in melanoma and breast carcinoma tissues.<sup>4,5</sup> Their presence correlated with increased tumor-infiltration of particular T-cell subsets which was shown to predict a favorable clinical outcome.<sup>4-7</sup> Hence, TLS create tumor-suppressing microenvironments by selectively facilitating T-cell influx, local T-cell priming and protective T-cell-mediated immune responses.<sup>8,9</sup>

LCH is a rare myeloid proliferative disorder with heterogeneous clinical manifestation and prognosis.<sup>10</sup> LCH can manifest as a single lesion or multiple lesions in one tissue type, i.e. single-system disease, or in multiple organ-systems: multi-system disease. LCH can affect every organ system in the body, from skin to visceral organs like spleen, liver and lungs, with the skeleton affected the most.<sup>10,11</sup> Typically, new LCH lesions other than the primary lesion may appear both during active disease (LCH progression) or after a period of non-active

disease (LCH reactivation).<sup>12,13</sup> To anticipate on this situation, accurate staging of the disease according to international clinical guidelines is highly recommended for all patients including those presenting with a single LCH lesion in skin or bone.<sup>10</sup>

Regardless of its clinical manifestation, all LCH lesions are comprised of CD1a<sup>+</sup> histiocytes which frequently carry somatic, cancer-associated BRAF<sup>V600E</sup> or MAP2K1 mutations.<sup>14-17</sup> These aberrant LCH-cells are intermixed with lymphoid cells, including various T-cell subsets.<sup>18-20</sup> Both lymphoid and myeloid cell types can be easily recognized in routinely prepared formalin-fixed paraffin-embedded (FFPE) and Hematoxylin/Eosin (H&E)-stained tissue sections. In the present study we analyzed the phenotype and organization of LCH-lesion-infiltrating immune cells and addressed, in retrospect, whether the presence of lymphoid aggregates at primary LCH onset affects the patients' risk of disease progression.

### Materials and methods

#### Patient materials

Archival LCH-affected FFPE-biopsies (bone ( $n = 71$ ), skin ( $n = 18$ ), lung ( $n = 13$ ) and bowel ( $n = 2$ )) collected from 104

**CONTACT** Astrid G. S. van Halteren  [a.g.s.van\\_halteren@lumc.nl](mailto:a.g.s.van_halteren@lumc.nl)

\*These authors equally contributed to this work.

© 2016 Willemijn T. Quispel, Eline C. Steenwijk, Vincent van Unen, Susy J. Santos, Lianne Koens, Reina Mebius, R. Maarten Egeler, and Astrid G. S. van Halteren. Published with license by Taylor & Francis Group, LLC.

This is an Open Access article distributed under the terms of the Creative Commons Attribution License (<http://creativecommons.org/licenses/by/3.0/>), which permits unrestricted use, distribution, and reproduction in any medium, provided the original work is properly cited. The moral rights of the named author(s) have been asserted.

**Table 1.** Patients demographics as analysed for lymphocyte aggregation, HEVs and TLS formation. \*One patient displayed the ARAF mutation.<sup>16</sup> \*\*One patient displayed a MAP2K1 mutation.<sup>17</sup> Other therapies is referred to as radiation therapy.

Variable	Hematoxylin & Eosin (n = 104)				MECA-79 (n = 77)			TLS (n = 15)	
	Total cohort (n = 104)	Scattered (n = 14)	Clustered (n = 56)	Lymphoid-follicular (n = 34)	Absent (n = 40)	Single cells (n = 21)	HEVs (n = 16)	Absent (n = 7)	Present (n = 8)
Sex, n (%)									
Female	29 (31)	4 (33)	16 (30)	9 (36)	9 (26)	6 (29)	5 (31)	4 (67)	2 (25)
Male	64 (69)	8 (67)	38 (70)	18 (64)	26 (64)	15 (71)	11 (69)	2 (33)	6 (75)
N.A.	11	2	2	7	5	0	0	1	0
Age at onset, n, median (range) in years									
< 18 y	70, 5 (0–17)	10, 6 (0–17)	43, 5 (0–17)	17, 4 (0–17)	30, 7 (0–17)	16, 3 (0–9)	14, 4 (0–17)	3, 6 (4–7)	3, 4 (0–17)
≥ 18 y	23, 37 (22–78)	2, 48 (47–48)	10, 37 (23–78)	11, 31 (22–66)	5, 28 (23–78)	5, 31 (27–54)	2, 31 (22–65)	2, 40 (27–53)	5, 31 (22–65)
N.A.	11	2	3	6	5	0	6	2	0
Manifestation, n (%)									
Mono-ostotic	48 (48)	9 (65)	27 (50)	12 (38)	26 (68)	10 (48)	6 (37)	5 (72)	5 (63)
Poly-ostotic	10 (10)	0	7 (13)	3 (10)	2 (5)	6 (29)	2 (13)	1 (14)	0
Multi-system	20 (20)	1 (7)	15 (27)	4 (13)	7 (18)	3 (14)	5 (31)	0	0
Single site skin	3 (3)	2 (14)	3 (5)	4 (13)	2 (5)	2 (9)	1 (6)	0	2 (25)
Pulmonary	13 (13)	2 (14)	3 (5)	8 (26)	1 (4)	0	2 (13)	1 (14)	1 (12)
N.A.	4	0	1	3	2	0	0	0	0
Mutation status, n (%)									
BRAF WT	31 (53)	3 (43)	19 (56)*	9 (53)**	13 (54)**	7 (47)	11 (73)*	1 (33)	4 (67)
BRAF V600E mutation	27 (47)	4 (57)	15 (44)	8 (47)	11 (66)	8 (53)	4 (27)	2 (67)	2 (33)
N.A.	46	7	22	17	16	6	1	4	2
Treatment, n (%)									
Biopsy with/without resection	30 (38)	3 (30)	15 (32)	12 (60)	8 (26)	7 (41)	5 (38)	0	1 (33)
Intralesional corticosteroid infiltration	27 (33)	5 (50)	16 (33)	6 (30)	14 (45)	6 (35)	3 (24)	3 (75)	2 (67)
Intralesional corticosteroid infiltration + other	4 (5)	0	2 (4)	2 (10)	2 (6)	1 (6)	0	1 (25)	0
Systemic steroids + chemotherapy	18 (23)	2 (20)	14 (29)	2 (10)	6 (20)	3 (18)	5 (38)	0	0
Systemic steroids + chemotherapy + other	1 (1)	0	1 (2)	0	1 (3)	0	0	0	0
N.A.	24	4	8	12	9	4	3	3	5
Appearance of new lesions, n (%)									
< 6 mo									
Yes	13 (15)	2 (22)	11 (22)	0	5 (15)	5 (25)	1 (6)	1 (25)	0
No	75 (85)	9 (78)	40 (78)	26 (100)	29 (85)	15 (75)	15 (94)	3 (75)	7 (100)
N.A.	16	3	5	8	6	1	0	3	1
≤ 2 y									
Yes	21 (24)	3 (27)	16 (29)	2 (23)	8 (18)	7 (35)	3 (23)	1 (25)	1 (12)
No	67 (76)	8 (73)	35 (71)	24 (77)	26 (82)	13 (65)	13 (77)	3 (75)	6 (88)
N.A.	16	3	5	8	6	1	0	3	1

patients at first disease manifestation were included in this study; patients' demographics are shown in Table 1. Additional analysis was performed on one skin and one bone lesion taken at of LCH progression/reactivation, but these samples were not included in correlation analysis. Data on LCH staging were available for 100 patients whereas data on LCH-progression and LCH-reactivation, assessed between 6 months and 2 years after LCH onset, were available for 88 out of 104 patients. In addition to normal skin and tonsillar tissue, a total of five LCH-affected LN served as controls.

The study was approved by the Institutional Review Board of the LUMC (P10.163) and was conducted following the ethical guidelines of the national organization of scientific societies (FEDERA).

### Immunohistochemistry, immunofluorescent staining and BRAF mutation analysis

Tissue sections were routinely H&E stained in a Leica St 5020 autostainer. Due to limited availability of tissue, the histological

workup for the presence of HEVs, TLS markers and mutations was performed on a selection of biopsies. The following primary (clone specified) and secondary antibodies were used in histochemical stainings:<sup>20,21</sup> CD1a (OIO), CD3, CD35 (Ber-MAC-DRC), CD79a (JCB117), BCL-6 (PG-B6p) (Dako, Glostrup, Denmark), CD25 (4C9), CD4 (1F6), CD8<sup>+</sup> (4B11), Langerin/CD207 (12D6) (Novocastra, Newcatle upon Tyne, UK), CD68 (514H12, AbD Serotec), CXCR5 (51505), CXCL13, CCL21 (all from R&D systems), FOXP3 (22510, Abcam, Cambridge, UK), Podoplanin (manufactured by Dr. H. Kawachi), HRP-labeled Brightvision goat-anti-rabbit-IgG mouse, donkey-anti-goat and Envision goat-anti-mouse (ImmunoLogic, Duiven, The Netherlands) and Alexa fluorochromes goat-anti-rat and goat-anti-mouse IgG2b-488 and goat-anti-rabbit-546 (Invitrogen, Carlsbad, CA, USA). Immunohistochemically-stained tissue sections were optically graded according to the cellular organization of the various cell types<sup>6</sup> by at least two individual researchers who were blinded for clinical data. Of note, lymphoid aggregates were defined as 'TLS-like structures or TLS' when they stained positively for CD3 and CD79 and, in

addition, for Bcl-6 or CD35.<sup>2</sup> Germinal center-like morphology was defined as a similar structural organization as can normally be found in lymphoid follicles present in LN, i.e. diffusely organized lymphocytes surrounded by densely packed lymphocytes. Lymphocyte aggregation has earlier been scored as radial lymphocyte count or, alternatively, to the presence of diffuse lymphocytes, germinal center or follicle-like morphology.<sup>22-27</sup> The criteria for the minimal number of scored cells varied however dramatically amongst these studies. This variation made it difficult to apply either methodology to our patient cohort. We therefore choose to score our samples according to the presence of diffuse cells<sup>27</sup> or follicle-like morphology<sup>22,23</sup> and added one other definition to describe an intermediate degree of lymphoid aggregation. When different stages of lymphoid aggregation were observed in the areas of CD1a<sup>+</sup> staining, we choose to define the biopsy according to the highest degree of lymphoid aggregation.

BRAF<sup>V600E</sup>-mutation analysis was performed on tissue sections subjected to microdissection or immunohistochemistry as previously described.<sup>14,28,29</sup> Note that this was done on a selection of cases (58/104) from whom sufficient tissue was left to cut minimally two consecutive 10  $\mu$ M sections.

### Statistical analysis

Statistical analysis was performed using SPSS version 20.0 and Prism 5.04 Software (Graphpad, La Jolla, CA, USA). Correlation analysis between the degree of lymphocyte aggregation, the presence of MECA-79 staining, the number of T-cell subsets and clinical parameters was performed using Mann-Whitney test, Fishers' Exact test, log rank-test and Kaplan Meier analysis. A *p* value of <0.05 was considered as statistically significant.

## Results

### Various stages of lymphoid aggregation are detected in LCH lesions

A randomly collected series of 104 archived H&E-stained LCH-affected tissue sections of non-lymphoid origin were scored according to the various degrees and number of lymphocyte aggregation. Tissue slides were classified as 'absent' when no organization or only scattered lymphocytes were observed, as in 13% of reviewed cases (14/104, Fig. 1A), as 'clustered' when lymphocytes were present in cellular clusters, as in 54% of cases (56/104), Fig. 1C) or as 'lymphoid-follicular' when lymphocytes were present at high densities and organized in one or more lymphoid-follicular structures. The latter were observed in 33% of biopsied tissues (34/104, Fig. 1E) wherein germinal center-like morphology could be visualized in 9/34 (26%) biopsies. The CD1a<sup>+</sup> LCH-cells were located either around or within the lymphocytes aggregates (Fig. 1B, D and F).

### HEVs are present in LCH lesions

HEVs mediate lymphocyte trafficking into secondary lymphoid organs and are often detected in TLS present in chronically inflamed tissues and tumor sites.<sup>3-5,30-34</sup> The antibody MECA-

79 recognizes peripheral lymph node addressins (PNAd) which are exclusively expressed by HEVs.<sup>35</sup> To identify the presence of HEVs in LCH lesions, immunohistochemical staining with MECA-79 was applied to a subset of biopsies (*n* = 77) which each displayed a defined form of lymphocyte aggregation being: scattered (*n* = 12), clustered (*n* = 44) or lymphoid-follicular (*n* = 21). Due to limited availability of tissue specimens, it was not possible to analyze the full sample collection. MECA-79 staining was detected in 37/77 (48%) lesions of which 16 lesions contained classically shaped HEVs i.e. venules lined with cubical endothelial cells (Fig. 2B).<sup>36</sup> These classical HEVs were located either within or in the perimeter of areas defined as clustered or lymphoid-follicular. HEVs were not observed in scattered biopsies. Eight tissues containing lymphoid-follicular aggregates as well as 26 clustered cases lacked, however, MECA-79 staining.

### Lymphoid-follicle aggregates represent TLS

A total of 15 samples were selected from which sufficient material was available for additional visualization of distinct markers classically associated with TLS-formation.<sup>21,37</sup> The selected samples represented all stages of lymphoid aggregation and included two samples with classical shaped HEVs, three samples with single MECA-79 cells and ten samples lacking MECA-79 positivity. We additionally analyzed one bone LCH lesion which was collected at LCH reactivation. Consistent with the key cell types typically located in normal LN,<sup>2</sup> LCH-associated TLS were composed of CD3<sup>+</sup> T- and CD79a<sup>+</sup> B-cells (Fig. 2D), CD35<sup>+</sup> FDC, Fig. 2I) and/or BCL-6-expressing cells (Fig. 2J). Of note, only germinal center-associated B-cells and B-cell lymphoma cells stain positive for BCL-6<sup>38</sup>. These phenotypically and structurally TLS-like lymphoid structures were present in 8/15 tissues of which 6/8 biopsies contained one or several lymphoid-follicular aggregates and 2/7 biopsies displayed absent or clustered lymphoid aggregation (*p* = 0.04). Classical HEVs were present in three samples that were classified as TLS-containing samples.

CCL21 and CXCL13 respectively control the segregation of CCR7<sup>+</sup> T-cells and CXCR5<sup>+</sup> B-cells within TLS.<sup>39,40</sup> CCL21 was detected in 7/15 biopsies, Fig. 2G) and CXCL13<sup>+</sup> cells were detected in 13 of 15 biopsies, Fig. 2F). Consistent with macrophages being CXCL13 producers,<sup>40</sup> CD68<sup>+</sup> macrophages were either concentrated around or within CXCL13 rich-areas (5/15, Fig. 2H). In contrast, 6/15 biopsies contained macrophages located in areas lacking CXCL13 or did not contain any macrophages (4/15). T- and B-cells were clearly separated in LCH-lesions expressing both chemokines which is visualized in Fig. 2D. CXCR5-positive cells co-localized with CD79a<sup>+</sup> B-cells in nine of the 15 biopsies (Fig. 2E). Also podoplanin-expressing FDC and fibroblastic reticular cells play crucial roles in T/B-cell compartmentalization (reviewed by<sup>3</sup>). Podoplanin staining was observed both within and around the lymphoid aggregates. Note that podoplanin<sup>+</sup> vessels (Fig. 2C) could be either HEVs, blood- or lymphatic vessels as this marker is not discriminative. Thus, T- and B-cell compartmentalization was most pronounced in LCH-lesions containing CXCL13<sup>+</sup>, CCL21<sup>+</sup> and podoplanin<sup>+</sup> cells.



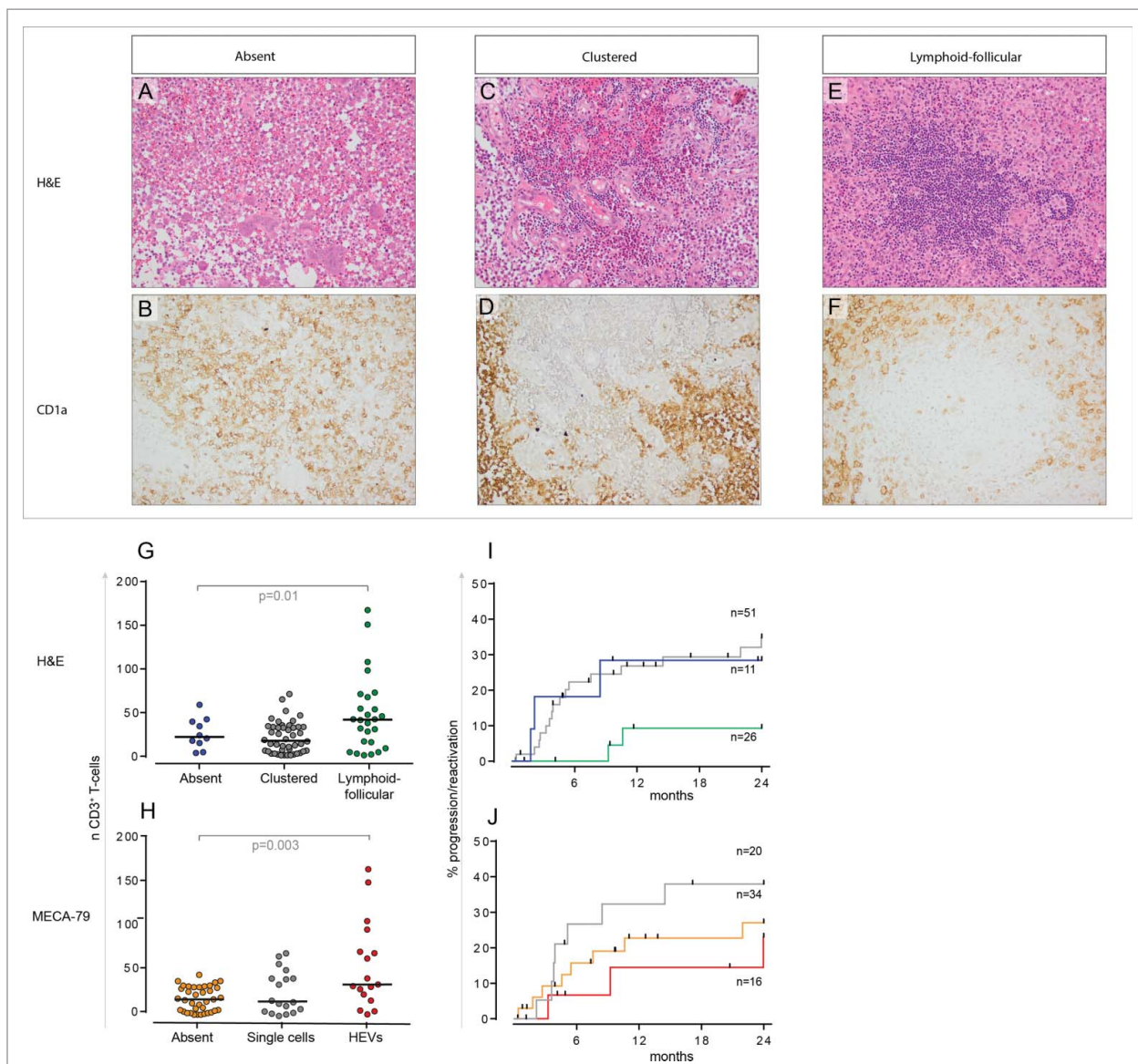


**Figure 1.** Various stages of lymphocyte aggregation in LCH-affected biopsies and correlation to clinical outcome. Representative pictures of the various stages of lymphoid aggregation in LCH-affected bone sections which were subjected to automated H&E staining (upper row, 20x) and manual immunohistochemical CD1a staining (bottom row, 20x). The bottom row shows the presence of LCH-cells in a subsequently cut tissue section. LCH lesions displayed either no organization of lymphocytes ('absent' as shown in A&B), moderate clustering of lymphocytes ('clustered' as shown in C&D) or high density of lymphocytes and similar organization as seen in normal lymphoid follicles ('lymphoid-follicular' as shown in E&F). Pictures were taken using a BX41 bright field microscope equipped with a UC30 camera (Olympus, Zoeterwoude, the Netherlands). Graphs showing the average number of single CD3<sup>+</sup> T-cells per microscopic field (40× original magnification) in relation to lymphoid aggregation detected on a serial H&E-stained tissue section (n = 81) (G) or to the presence of MECA-79<sup>+</sup> HEVs (n = 72) as assessed in parallel section stained with MECA-79 (H). Kaplan-Meier plot in (I) shows the percentage of patients where a new lesion appeared in relation to lymphoid organization of their LCH lesion assessed at disease onset (n = 88). Kaplan-Meier plot in (J) shows the percentage of patients who displayed progression or reactivation in relation to the presence of MECA-79 staining in their LCH lesion assessed at disease onset (n = 70). Note that these survival data were not corrected for treatment modality which, if any, was started after the analyzed biopsy was taken.

### **BRAF mutation status does not affect the degree of lymphoid organization**

As recently proposed, unifocal LCH lesions are possibly the result of somatic mutations which occur *in situ*.<sup>41-43</sup> To assess whether BRAF-mutation status of lesional LCH-cells influences the degree of lymphoid aggregation, we analysed the presence of BRAF<sup>V600E</sup> mutation in CD1a-enriched tissue derived from the same tissue block as was used for lymphoid aggregation analysis (n = 58). The presence of BRAF<sup>V600E</sup> expressing LCH-cells (n = 27) did not correlate with the degree of lymphoid aggregation ( $p = 0.81$ , data

not shown). Likewise, the presence of HEVs did not correlate with the presence of BRAF<sup>V600E</sup> expressing LCH-cells ( $p = 0.28$ , data not shown).

### **The highest number of T-cells are detected in tissues which display the highest degrees of lymphoid aggregation and HEVs**

Previous findings demonstrate that lymphocytes are present in variable numbers in LCH lesions as highly frequently described in routine pathology reports.<sup>18-20</sup> HEVs mediate lymphocyte

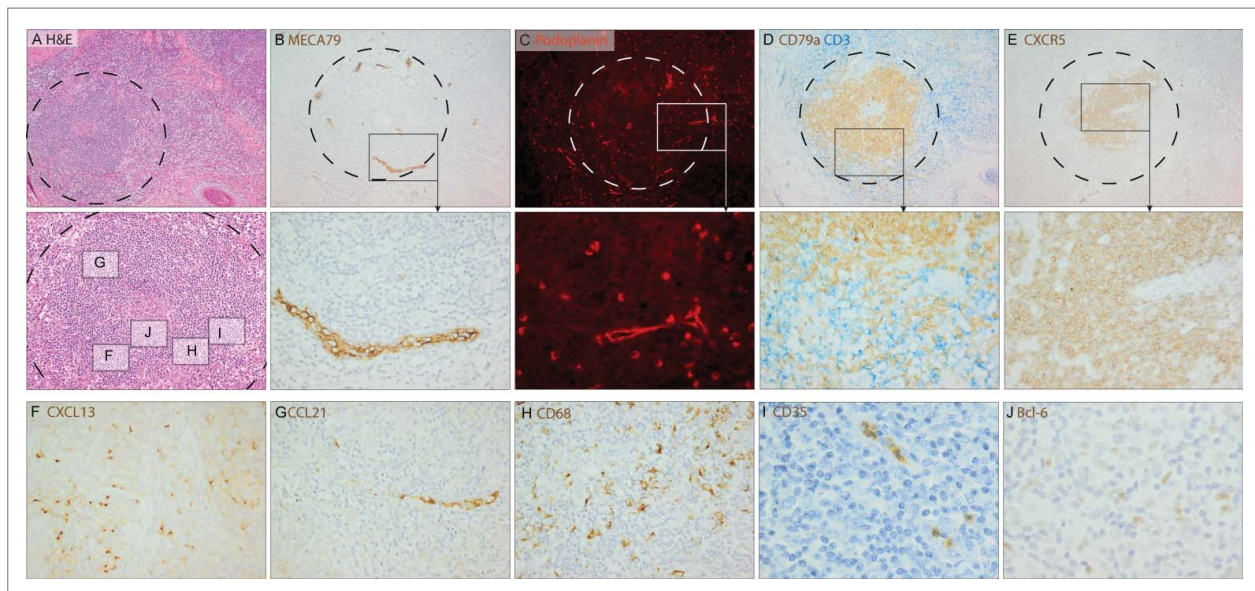


**Figure 2.** Immunofluorescent and immunohistochemical staining of classical TLS-inducing factors visualized in an isolated skin LCH lesion containing the highest degree of TLS formation. Representative pictures were taken at 20°C using a Leica DM5500B fluorescence microscope equipped with a DFC-350-FX camera (40x original magnification) or a Olympus BX41 bright field microscope equipped with a UC30 camera (original magnification 10x (upper row), 20x (middle row and F–H) and 40x (I–J)). Middle row photographs are a larger magnification of the cells in the indicated areas of the upper row pictures. Photographs F–J were taken from the indicated areas depicted in the larger magnification of A. Pictures from left to right from top to bottom showing the key cell types which are typically located in normal LN that is: a lymphoid-follicular aggregate on H&E (A), MECA-79-expressing HEVs (B), Podoplanin<sup>+</sup> single cells (red color and box) as well as Podoplanin<sup>+</sup> vessels (C), segregated CD3<sup>+</sup> T-cells (blue)- and CD79a<sup>+</sup> B-cells (brown) (D), the B-cell-organogenic chemokine/chemokine receptor pair, CXCR5 (E) and CXCL13 (F), the T-cell organogenic chemokine CCL21 (G), CD68<sup>+</sup> macrophages (H), CD35<sup>+</sup> FDC (I) and centrally located BCL-6-expressing cells (J). No immunoreactivity was detected for any type of secondary antibodies when consecutive sections were stained with the secondary antibodies only (Fluorochromes 488, 546 and 647).<sup>21,37</sup> Negative controls were stained in parallel with the same secondary reagents, but the primary antibodies were omitted (data not shown).

recruitment into secondary lymphoid organs as well as chronically inflamed non-lymphoid tissues.<sup>4,5,30–34</sup> Indeed, HEV-expressing LCH-lesions contained higher absolute numbers of CD3<sup>+</sup> T-cells ( $p = 0.003$ , Fig. 1H), CD4<sup>+</sup> FOXP3<sup>−</sup> T-helper cells ( $p = 0.03$ ) and CD4, CD25 and FOXP3 co-expressing T-reg ( $p = 0.03$ ). Moreover, lesion-infiltrating CD3<sup>+</sup> T-cells ( $p = 0.01$ , Fig. 1G), CD4<sup>+</sup> FOXP3<sup>−</sup> T-helper cells ( $p = 0.002$ ) and CD25<sup>+</sup> FOXP3<sup>+</sup> regulatory T-cells (T-reg) ( $p = 0.009$ ) were more prevalent in lesions containing the highest degree of lymphocyte aggregation as compared to the lowest level of aggregation.

Besides facilitating PNAd-mediated lymphocyte entry, HEVs also recruit B- and T-cells through the release and/or presentation of chemo-attractant molecules such as CXCL13 and CCL21, respectively.<sup>5,31,32,34</sup> CCL21 was detected in 7/15 biopsies (47%) of which two LCH lesions clearly contained CCL21-expressing vascular structures (Fig. 2G).

### **LCH patients with lymphoid-follicle aggregates are less prone to develop new LCH lesions**

We next evaluated the putative prognostic value of lymphoid aggregation and MECA-79 staining at LCH onset in 88 patients. In analogy to other reports,<sup>22–27</sup> we compared the outcome between patients who initially presented with diffuse lymphocytes versus lymphoid-follicular aggregates. Unfortunately, information on therapy duration and the appearance of new LCH lesion is often poorly documented in hospital records. New lesions may appear either during therapy (LCH progression) or after a disease-free period (LCH reactivation). We therefore choose to register the appearance of each new lesion within respectively 6 months and 2 years after first onset

of LCH as an event. Within 6 months from diagnosis, new LCH lesions appeared in two out of 11 patients (18%) who displayed scattered lymphocytes at LCH onset in comparison to 0/26 patients (0%) who clearly displayed lymphoid-follicular aggregates in their biopsied lesion (Fig. 1I, Table 1,  $p = 0.04$ ). After 2 years of follow-up, new lesions had appeared in 3/11 (27%) of the patients without lymphocyte organization in comparison to 2/26 (8%) in patients with lymphoid-follicular structures in their diagnostic biopsy (Fig. 1I, Table 1,  $p = 0.09$ ).

Within 6 mo from diagnosis, new LCH lesions appeared in 5/34 (15%) patients without MECA-79 positivity in their biopsy in comparison to 1/16 (6%) patients with MECA-79<sup>+</sup> HEVs in their biopsied lesion ( $p = 0.34$ ). After 2 y of follow-up, new lesions had appeared in 8/34 (23%) patients without MECA-79 positive cells in comparison to 3/16 (19%) patients with HEVs in their diagnostic biopsy (Fig. 1J, Table 1,  $p = 0.5$ ).

### **Lymphoid-follicle aggregates are confined to patients with unifocal LCH**

Previous epidemiologic studies have shown that LCH reactivation is related to LCH manifestation at LCH onset.<sup>44,45</sup> In our study, the appearance of new lesions was significantly higher in patients who initially presented with multiple LCH lesions (14/29, 48%) than in patients with unifocal LCH (11/57, 19%) ( $p = 0.02$ ). We therefore assessed whether lymphoid-follicle aggregates or HEVs were found more frequently in patients with the lowest risk to develop new lesions in  $n = 100$  correctly staged patients. Lymphoid-follicular aggregates were indeed more prevalent in patients who presented with unifocal LCH (24/70, 34%) than in patients diagnosed with multiple



lesions (7/30, 23%  $p = 0.03$ ). The frequency of classical-shaped HEVs was not different between unifocal and multifocal LCH (9/50, 18% versus 7/25, 28%,  $p = 0.36$ ). Hence, in this small group of patients, highly organized lymphoid aggregation at LCH onset seems to correlate with unifocal LCH and to reduce the patient's risk to develop new LCH lesions within the first 2 years after first LCH onset.

## Discussion

LCH lesions are characterized by tissue accumulating LCH-cells along with the concurrent infiltration of various types of immune cells. Limited research has focused on the individual contribution of these leukocytes, being mainly lymphocytes and macrophages, to LCH outcome.<sup>18-20,46,47</sup> The *in situ* presence and organization of lymphoid cells in LCH-affected tissues has not been investigated yet. In this study, we demonstrate that various stages of lymphoid aggregation are detected in LCH lesions. The highest degree of aggregation, lymphoid-follicle aggregation, was confined to patients with unifocal LCH and the highest influx of absolute numbers of CD3<sup>+</sup> T-cells. Moreover, patients with lymphoid-follicle-containing lesions had the lowest risk to develop additional LCH lesions.

One of the limitations of performing research on archived tissue specimens is the often limited clinical information regarding staging, therapy duration and follow-up of the patients. This may lead to underestimation of the incidence of multifocal or multi-system patients and hampers proper differentiation between disease progression and reactivation. Correct staging of poly-ostotic patients in particular, may reveal the involvement of other non-ostotic tissues and designate them as multi-system patient. This may explain our observation that patients with multifocal LCH (comprised of poly-ostotic and multi-system LCH), and not solely multi-system patients, had a higher risk to develop new lesions. Highly organized lymphoid aggregation at LCH onset seems to reduce the patient's risk to develop new LCH lesions within 2 years from diagnosis. Whether the combination of lymphoid-follicle aggregates and HEVs lead to a better outcome could not be assessed due to the relative small sample size in this study. Such a study could be feasible but requires a multicenter set up and excess to detailed clinical record files.

TLS are dynamic and plastic structures,<sup>48,49</sup> which is illustrated by the reduction of lymphoid aggregation after TNF blockade in rheumatoid arthritis and psoriatic arthritis patients.<sup>50</sup> The various stages of lymphoid aggregation, TLS and the differential MECA-79 staining patterns found in LCH patients underlines the plasticity of the lymphoid aggregates. Based on the lack of correlation with BRAF mutation status, lymphoid aggregation in LCH is more likely organized by stromal factors rather than by the genotypically aberrant LCH-cells.<sup>3,24</sup> In line with observations in melanoma patients,<sup>48</sup> some large LCH biopsies contained aggregates with different stages of TLS development, ranging from large lymphoid aggregates, which stained positive for all TLS markers, to scattered B- and T-cells. We could therefore speculate that the extent of lymphoid aggregation as seen in biopsies taken at LCH-diagnosis does not necessarily reflect the final result of the process of lymphoid aggregation. When untouched, scattered lymphocytes may further develop into highly organized and functional TLS.

As shown previously, LCH lesions contain various types of activated T-cell subsets.<sup>18,20</sup> The presence of these conventional T-cells and T-reg has been confirmed in the present study. In addition, we demonstrate the presence of CD79a<sup>+</sup> B-cells, while B-cells and plasma cells have only been reported in a small number of cases.<sup>51</sup> T- and B-cell compartmentalization was most pronounced in LCH-lesions containing CXCL13<sup>+</sup>, CCL21<sup>+</sup> and podoplanin<sup>+</sup> cells. This is in accordance with previously published data demonstrating that these factors induce distinct T- and B-cell zones.<sup>3,31,33,39,40,52</sup>

In line with the lymphocyte recruitment capacity of HEVs, HEV-expressing LCH-lesions contained higher absolute numbers of all CD3<sup>+</sup> T-cells and conventional CD4<sup>+</sup> FOXP3<sup>-</sup> T-helper cells; B-cell influx was not assessed. This positive correlation has also been reported in various malignancies.<sup>3,4,52,53</sup> In addition, the presence of HEVs also correlated with high numbers of LCH-lesion-infiltrating CD4, CD25 and FOXP3 co-expressing T-reg ( $p = 0.04$ ). This finding is in contrast to melanomas where lower numbers of T-reg were reported to infiltrate HEVs-expressing lesions.<sup>5</sup> Hence, LCH-associated HEVs seem to facilitate the entry of various types of T-cells into LCH-lesions. The rarely observed expression of CCL21 on intra-lesional vasculature could explain the observed lack of correlation between the number of LCH-lesion-infiltrating T-cells and intralesional production of CCL21 ( $p = 0.39$ ). Nonetheless, combined expression of MECA-79 and CCL21 could further enhance the influx of T-cells, as has been observed in murine models of melanoma and lung carcinoma.<sup>8</sup> The observed correlation between the presence of lymphoid-follicular aggregates, HEVs and increased lymphocyte infiltration (Fig. 1G-H), suggests that LCH lesions may be successfully eradicated by local promotion of T effector T-cell influx and subsequent activation. This phenomenon has been described in lung cancer and melanoma patients.<sup>6,7</sup> In fact, self-regressing LCH lesions have been reported and unifocal LCH bone lesions are often not treated because it is well accepted that these lesions often spontaneously regress after a biopsy is taken.<sup>54</sup> We also analysed two tissue samples that were taken from a newly appearing lesion; biopsies from the same patients collected at first disease onset were, unfortunately, not available. The newly formed lesions of both patients contained HEVs and the one analyzed for TLS markers was classified as a TLS-containing lesion. Interestingly, both patients never developed additional lesions in time (follow-up between 14 and 25 years). As documented in their records, both secondary LCH lesions were biopsied without any further topical treatment, suggesting that the co-presence of TLS and HEVs may facilitate successful elimination of the disease.

For "non-central-nervous-system risk" mono-ostotic lesions curettage and a watchful waiting approach is often used as these patients have an excellent prognosis.<sup>45</sup> Clinical experience in LCH has nonetheless shown that corticosteroids are often deposited at the biopsied site. This treatment may be beneficial for painful, non-regressing mono-ostotic lesions. However, corticosteroids suppress immune function in several ways and induced the disappearance of fully functional TLS.<sup>50,55</sup> Based on these data and the putative beneficial effects of follicular aggregates for early disease control in LCH, it is questionable whether standard intralesional corticosteroid infiltration is justified in all

unifocal bone lesions which appear at other sites than the craniofacial bones ('special site'). Whether a quick scan for the presence of lymphocyte aggregation in a H&E-stained tissue section prepared from a snap-frozen tissue biopsy may facilitate this decision should be validated in a prospective study. In the present cohort, the presence of TLS correlated with the degree of lymphoid aggregation ( $p=0.04$ ). As lymphoid-follicular aggregates are simply detected at low power magnification in H&E-stained sections (Fig. 1), it would not be necessary to stain every LCH lesion collected at diagnosis for each distinct TLS marker set as depicted in Fig. 2. We acknowledge, however, that defining the presence of HEVs in a MECA-79 staining is less subjective than screening H&E samples for lymphoid aggregation. Furthermore, we suggest the use of an objective assessment method such as digital morphometric studies which may provide more objective data on the degree of lymphoid aggregation and quantification of infiltrating T-cells.

### Disclosure of potential conflicts of interest

No potential conflicts of interest were disclosed.

### Acknowledgements

We thank Prof. Dr J.V.M.G. Bovée, Dr R. van Eijk, B. van den Akker, Dr M. E. Penning and Dr J.J. Baelde (Department of Pathology, Leiden University Medical Center) for providing archived tissue samples, Podoplanin-specific antibody (which was manufactured by Dr H. Kawachi, Niigata University School of Medicine, Niigata, Japan) and technical support on BRAF genotyping. Dr C. van den Bos (Dept. of Pediatric Oncology, Emma Kinderziekenhuis/Amsterdam Medical Center) is acknowledged for providing tissue samples and clinical information.

### Funding

This work was supported by the "1000 kaarsjes voor Juultje" Foundation, which had no role in the collection, analysis or interpretation of presented data.

### Author contributions

Contribution: W.T.Q.— study design, literature search, data collection and interpretation, writing the paper; V.U., E.S., S.J.S. and L.K.—data collection; L.K. and R.M.—provided reagents and data interpretation; R.M.E.—overall clinical leader; A.G.S.H.—senior of technical aspects in the lab, study design, sample collection, data collection and interpretation, writing the manuscript.

### References

- Kratz A, Campos-Neto A, Hanson MS, Ruddle NH. Chronic inflammation caused by lymphotoxin is lymphoid neogenesis. *J Exp Med* 1996; 183:1461-72; PMID:8666904; <http://dx.doi.org/10.1084/jem.183.4.1461>
- Pabst R. Plasticity and heterogeneity of lymphoid organs. What are the criteria to call a lymphoid organ primary, secondary or tertiary? *Immunol Lett* 2007; 112:1-8; PMID:17698207; <http://dx.doi.org/10.1016/j.imlet.2007.06.009>
- Stranford S, Ruddle NH. Follicular dendritic cells, conduits, lymphatic vessels, and high endothelial venules in tertiary lymphoid organs: Parallels with lymph node stroma. *Front Immunol* 2012; 3:350; PMID:23230435; <http://dx.doi.org/10.3389/fimmu.2012.00350>
- Martinet L, Garrido I, Filleron T, Le Guellec S, Bellard E, Fournie JJ, Rochaix P, Girard JP. Human solid tumors contain high endothelial venules: association with T- and B-lymphocyte infiltration and favorable prognosis in breast cancer. *Cancer Res* 2011; 71:5678-87; PMID:21846823; <http://dx.doi.org/10.1158/0008-5472.CAN-11-0431>
- Martinet L, Le Guellec S, Filleron T, Lamant L, Meyer N, Rochaix P, Garrido I, Girard JP. High endothelial venules (HEVs) in human melanoma lesions: Major gateways for tumor-infiltrating lymphocytes. *Oncoimmunology* 2012; 1:829-39; PMID:23162750; <http://dx.doi.org/10.4161/onci.20492>
- Clemente CG, Mihm MC Jr, Bufalino R, Zurrida S, Collini P, Cascinelli N. Prognostic value of tumor infiltrating lymphocytes in the vertical growth phase of primary cutaneous melanoma. *Cancer* 1996; 77:1303-10; PMID:8608507; [http://dx.doi.org/10.1002/\(SICI\)1097-0142\(19960401\)77:7<1303::AID-CNCR12>3.0.CO;2-5](http://dx.doi.org/10.1002/(SICI)1097-0142(19960401)77:7<1303::AID-CNCR12>3.0.CO;2-5)
- Goc J, Fridman WH, Hammond SA, Sautes-Fridman C, Dieu-Nosjean MC. Tertiary lymphoid structures in human lung cancers, a new driver of antitumor immune responses. *Oncoimmunology* 2014; 3:e28976; PMID:25083325; <http://dx.doi.org/10.4161/onci.28976>
- Peske JD, Thompson ED, Gemta L, Baylis RA, Fu YX, Engelhard VH. Effector lymphocyte-induced lymph node-like vasculature enables naive T-cell entry into tumours and enhanced anti-tumour immunity. *Nat Commun* 2015; 6:7114; PMID:25968334; <http://dx.doi.org/10.1038/ncomms8114>
- Thompson ED, Enriquez HL, Fu YX, Engelhard VH. Tumor masses support naive T cell infiltration, activation, and differentiation into effectors. *J Exp Med* 2010; 207:1791-804; PMID:20660615; <http://dx.doi.org/10.1084/jem.20092454>
- Haupt R, Minkov M, Astigarraga I, Schäfer E, Nanduri V, Jubran R, Egeler RM, Janka G, Micic D, Rodriguez-Galindo C et al. Langerhans cell histiocytosis (LCH): guidelines for diagnosis, clinical work-up, and treatment for patients till the age of 18 years. *Pediatr Blood Cancer* 2013; 60:175-84; PMID:23109216; <http://dx.doi.org/10.1002/pbc.24367>
- Satter EK, High WA. Langerhans cell histiocytosis: a review of the current recommendations of the Histiocyte Society. *Pediatr Dermatol* 2008; 25:291-5; PMID:18577030; <http://dx.doi.org/10.1111/j.1525-1470.2008.00669.x>
- Gadner H, Minkov M, Grois N, Pötschger U, Thiem E, Aric M, Astigarraga I, Braier J, Donadieu J, Henter JI et al. Therapy prolongation improves outcome in multisystem Langerhans cell histiocytosis. *Blood* 2013; 121:5006-14; PMID:23589673; <http://dx.doi.org/10.1182/blood-2012-09-455774>
- Pollono D, Rey G, Latella A, Rosso D, Chantada G, Braier J. Reactivation and risk of sequelae in Langerhans cell histiocytosis. *Pediatr Blood Cancer* 2007; 48:696-9; PMID:17252574; <http://dx.doi.org/10.1002/pbc.21145>
- Badalian-Very G, Vergilio JA, Degar BA, MacConaill LE, Brandner B, Calicchio ML, Kuo FC, Ligon AH, Stevenson KE, Kehoe SM et al. Recurrent BRAF mutations in Langerhans cell histiocytosis. *Blood* 2010; 116:1919-23; PMID:20519626; <http://dx.doi.org/10.1182/blood-2010-04-279083>
- Brown NA, Furtado LV, Betz BL, Kiel MJ, Weigelin HC, Lim MS, Elenitoba-Johnson KS. High prevalence of somatic MAP2K1 mutations in BRAF V600E negative Langerhans cell histiocytosis. *Blood* 2014; 124:1655-8; PMID:24982505; <http://dx.doi.org/10.1182/blood-2014-05-577361>
- Nelson DS, Quispel W, Badalian-Very G, van Halteren AG, van den Bos C, Bovée JV, Tian SY, Van Hummelen P, Ducar M, MacConaill LE et al. Somatic activating ARAF mutations in Langerhans cell histiocytosis. *Blood* 2014; 123:3152-5; PMID:24652991; <http://dx.doi.org/10.1182/blood-2013-06-511139>
- Nelson DS, van Halteren A, Quispel WT, van den Bos C, Bovée JV, Patel B, Badalian-Very G, van Hummelen P, Ducar M, Lin L, MacConaill LE, Egeler RM, Rollins BJ. 54(6):361-8; PMID:25899310; <http://dx.doi.org/10.1002/gcc.22247>
- Senechal B, Elain G, Jeziorski E, Grondin V, Patey-Mariaud de Serre N, Jaubert F, Beldjord K, Lellouch A, Glorion C, Zerah M et al. Expansion of regulatory T cells in patients with Langerhans cell histiocytosis. *PLoS Med* 2007; 4:e253; PMID:17696642; <http://dx.doi.org/10.1371/journal.pmed.0040253>

19. Egeler RM, Favara BE, van Meurs M, Laman JD, Claassen E. Differential In situ cytokine profiles of Langerhans-like cells and T cells in Langerhans cell histiocytosis: abundant expression of cytokines relevant to disease and treatment. *Blood* 1999; 94:4195-201.
20. Quispel WT, Stegehuis-Kamp JA, Santos SJ, Egeler RM, Halteren van AGS. Activated conventional T-cells are present in Langerhans Cell Histiocytosis lesions despite the presence of immune suppressive cytokines. *J Interferon Cytokine Res* 2015.
21. Koenigs L, Senff NJ, Vermeer MH, Willemze R, Jansen PM. Methotrexate-associated B-cell lymphoproliferative disorders presenting in the skin: A clinicopathologic and immunophenotypic study of 10 cases. *Am J Surg Pathol* 2014; 38:999-1006; PMID:24805861; <http://dx.doi.org/10.1097/PAS.0000000000000225>
22. Freni MA, Artuso D, Gerken G, Spanti C, Marafioti T, Alessi N, Spadaro A, Ajello A, Ferrau O. Focal lymphocytic aggregates in chronic hepatitis C: occurrence, immunohistochemical characterization, and relation to markers of autoimmunity. *Hepatology* 1995; 22:389-94; PMID:7635405; <http://dx.doi.org/10.1002/hep.1840220203>
23. Salomonsson S, Jonsson MV, Skarstein K, Brokstad KA, Hjelmström P, Wahren-Herlenius M, Jonsson R. Cellular basis of ectopic germinal center formation and autoantibody production in the target organ of patients with Sjogren's syndrome. *Arthritis Rheum* 2003; 48:3187-201; PMID:14613282; <http://dx.doi.org/10.1002/art.11311>
24. Barone F, Bombardieri M, Manzo A, Blades MC, Morgan PR, Challacombe SJ, Valesini G, Pitzalis C. Association of CXCL13 and CCL21 expression with the progressive organization of lymphoid-like structures in Sjogren's syndrome. *Arthritis Rheum* 2005; 52:1773-84; PMID:15934082; <http://dx.doi.org/10.1002/art.21062>
25. Canete JD, Santiago B, Cantaert T, Sanmartí R, Palacin A, Celis R, Graell E, Gil-Torregrosa B, Baeten D, Pablos JL. Ectopic lymphoid neogenesis in psoriatic arthritis. *Ann Rheum Dis* 2007; 66:720-6; PMID:17223654; <http://dx.doi.org/10.1136/ard.2006.062042>
26. Kirsh AL, Cushing SL, Chen EY, Schwartz SM, Perkins JA. Tertiary lymphoid organs in lymphatic malformations. *Lymphat Res Biol* 2011; 9:85-92; PMID:21688977; <http://dx.doi.org/10.1089/lrb.2010.0018>
27. Mittal S, Revell M, Barone F, Hardie DL, Matharu GS, Davenport AJ, Martin RA, Grant M, Mosselmanns F, Pynsent P et al. Lymphoid aggregates that resemble tertiary lymphoid organs define a specific pathological subset in metal-on-metal hip replacements. *PLoS One* 2013; 8: e63470; PMID:23723985; <http://dx.doi.org/10.1371/journal.pone.0063470>
28. van Eijk R, Stevens L, Morreau H, van Wezel T. Assessment of a fully automated high-throughput DNA extraction method from formalin-fixed, paraffin-embedded tissue for KRAS, and BRAF somatic mutation analysis. *Exp Mol Pathol* 2013; 94:121-5; PMID:22750048; <http://dx.doi.org/10.1016/j.yexmp.2012.06.004>
29. Sahn F, Capper D, Preusser M, Meyer J, Stenzinger A, Lasitschka F, Berghoff AS, Habel A, Schneider M, Kulozik A et al. BRAFV600E mutant protein is expressed in cells of variable maturation in Langerhans cell histiocytosis. *Blood* 2012; 120:e28-e34; PMID:22859608; <http://dx.doi.org/10.1182/blood-2012-06-429597>
30. Girard JP, Moussion C, Forster R. HEVs, lymphatics and homeostatic immune cell trafficking in lymph nodes. *Nat Rev Immunol* 2012; 12:762-73; PMID:23018291; <http://dx.doi.org/10.1038/nri3298>
31. de Chaisemartin L, Goc J, Damotte D, Validire P, Magdeleinat P, Aliano M, Cremer I, Fridman WH, Sautès-Fridman C, Dieu-Nosjean MC et al. Characterization of chemokines and adhesion molecules associated with T cell presence in tertiary lymphoid structures in human lung cancer. *Cancer Res* 2011; 71:6391-9; PMID:21900403; <http://dx.doi.org/10.1158/0008-5472.CAN-11-0952>
32. Miyasaka M, Tanaka T. Lymphocyte trafficking across high endothelial venules: dogmas and enigmas. *Nat Rev Immunol* 2004; 4:360-70; PMID:15122201; <http://dx.doi.org/10.1038/nri1354>
33. Aloisi F, Pujol-Borrell R. Lymphoid neogenesis in chronic inflammatory diseases. *Nat Rev Immunol* 2006; 6:205-17; PMID:16498451; <http://dx.doi.org/10.1038/nri1786>
34. Girard JP, Springer TA. High endothelial venules (HEVs): specialized endothelium for lymphocyte migration. *Immunol Today* 1995; 16:449-57; PMID:7546210; [http://dx.doi.org/10.1016/0167-5699\(95\)80023-9](http://dx.doi.org/10.1016/0167-5699(95)80023-9)
35. Hemmerich S, Butcher EC, Rosen SD. Sulfation-dependent recognition of high endothelial venules (HEV)-ligands by L-selectin and MECA 79, and adhesion-blocking monoclonal antibody. *J Exp Med* 1994; 180:2219-26; PMID:7525849; <http://dx.doi.org/10.1084/jem.180.6.2219>
36. Mebius RE, Bauer J, Twisk AJ, Breave J, Kraal G. The functional activity of high endothelial venules: a role for the subcapsular sinus macrophages in the lymph node. *Immunobiology* 1991; 182:277-91; PMID:1833312.
37. Quispel WT, Stegehuis-Kamp JA, Santos SJ, van Wengen A, Dompeling E, Egeler RM, van de Vosse E, van Halteren AG. Intact IFN-gammaR1 expression and function distinguishes Langerhans cell histiocytosis from mendelian susceptibility to mycobacterial disease. *J Clin Immunol* 2014; 34:84-93; PMID:24254535; <http://dx.doi.org/10.1007/s10875-013-9959-1>
38. Jardin F, Ruminy P, Bastard C, Tilly H. The BCL6 proto-oncogene: a leading role during germinal center development and lymphomagenesis. *Pathol Biol (Paris)* 2007; 55:73-83; PMID:16815642; <http://dx.doi.org/10.1016/j.patbio.2006.04.001>
39. Luther SA, Bidgol A, Hargreaves DC, Schmidt A, Xu Y, Paniyadi J, Matloubian M, Cyster JG. Differing activities of homeostatic chemokines CCL19, CCL21, and CXCL12 in lymphocyte and dendritic cell recruitment and lymphoid neogenesis. *J Immunol* 2002; 169:424-33; PMID:12077273; <http://dx.doi.org/10.4049/jimmunol.169.1.424>
40. Carlsen HS, Baekkevold ES, Morton HC, Haraldsen G, Brandtzaeg P. Monocyte-like and mature macrophages produce CXCL13 (B cell-attracting chemokine 1) in inflammatory lesions with lymphoid neogenesis. *Blood* 2004; 104:3021-7; PMID:15284119; <http://dx.doi.org/10.1182/blood-2004-02-0701>
41. Allen CE, Li L, Peters TL, Leung HC, Yu A, Man TK, Gurusiddappa S, Phillips MT, Hicks MJ, Gaikwad A et al. Cell-specific gene expression in Langerhans cell histiocytosis lesions reveals a distinct profile compared with epidermal Langerhans cells. *J Immunol* 2010; 184:4557-67; PMID:20220088; <http://dx.doi.org/10.4049/jimmunol.0902336>
42. Berres ML, Lim KP, Peters T, Price J, Takizawa H, Salmon H, Idoyaga J, Ruza A, Lupo PJ, Hicks MJ et al. BRAF-V600E expression in precursor versus differentiated dendritic cells defines clinically distinct LCH risk groups. *J Exp Med* 2014; 211:669-83; PMID:24638167; <http://dx.doi.org/10.1084/jem.20130977>
43. Berres ML, Merad M, Allen CE. Progress in understanding the pathogenesis of Langerhans cell histiocytosis: back to Histiocytosis X? *Br J Haematol* 2014; 169(1):3-3; PMID:25430560; <http://dx.doi.org/10.1111/bjh.13247>
44. Minkov M. Multisystem Langerhans cell histiocytosis in children: current treatment and future directions. *Paediatr Drugs* 2011; 13:75-86; PMID:21351807; <http://dx.doi.org/10.2165/11538540-00000000-000000>
45. Weitzman S, Egeler RM. Langerhans cell histiocytosis: update for the pediatrician. *Curr Opin Pediatr* 2008; 20:23-9; PMID:18197035; <http://dx.doi.org/10.1097/MOP.0b013e3282f45ba4>
46. Ohnishi K, Komohara Y, Sakashita N, Iyama K, Murayama T, Takeya M. Macrophages in Langerhans cell histiocytosis are differentiated toward M2 phenotype: their possible involvement in pathological processes. *Pathol Int* 2010; 60:27-34; PMID:20055949; <http://dx.doi.org/10.1111/j.1440-1827.2009.02472.x>
47. Gatalica Z, Bilalovic N, Palazzo JP, Bender RP, Swensen J, Millis SZ, Vranic S, Von Hoff D, Arcenci RJ. Disseminated histiocytoses biomarkers beyond BRAFV600E: frequent expression of PD-L1. *Oncotarget* 2015; 6:19819-25; PMID:26110571; <http://dx.doi.org/10.18632/oncotarget.4378>
48. Cipponi A, Mercier M, Seremet T, Baurain JF, Théate I, van den Oord J, Stas M, Boon T, Coulie PG, van Baren N. Neogenesis of lymphoid structures and antibody responses occur in human melanoma metastases. *Cancer Res* 2012; 72:3997-4007; PMID:22850419; <http://dx.doi.org/10.1158/0008-5472.CAN-12-1377>
49. Hjelmstrom P. Lymphoid neogenesis: de novo formation of lymphoid tissue in chronic inflammation through expression of homing chemokines. *J Leukoc Biol* 2001; 69:331-9; PMID:11261778



50. Klaasen R, Thurlings RM, Wijbrandts CA, van Kuijk AW, Baeten D, Gerlag DM, Tak PP. The relationship between synovial lymphocyte aggregates and the clinical response to infliximab in rheumatoid arthritis: a prospective study. *Arthritis Rheum* 2009; 60:3217-24; PMID:19877042; <http://dx.doi.org/10.1002/art.24913>
51. Jeziorski E, Senechal B, Molina TJ, Devez F, Leruez-Ville M, Morand P, Glorion C, Mansuy L, Gaudelus J, Debre M et al. Herpes-virus infection in patients with Langerhans cell histiocytosis: a case-controlled sero-epidemiological study, and in situ analysis. *PLoS One* 2008; 3:e3262; PMID:18810271; <http://dx.doi.org/10.1371/journal.pone.0003262>
52. Goc J, Fridman WH, Sautès-Fridman C, Dieu-Nosjean MC. Characteristics of tertiary lymphoid structures in primary cancers. *Oncoimmunology* 2013; 2:e26836; PMID:24498556; <http://dx.doi.org/10.4161/onci.26836>
53. Fridman WH, Remark R, Goc J, Giraldo NA, Becht E, Hammond SA, Damotte D, Dieu-Nosjean MC, Sautès-Fridman C. The immune microenvironment: a major player in human cancers. *Int Arch Allergy Immunol* 2014; 164:13-26; PMID:24852691; <http://dx.doi.org/10.1159/000362332>
54. Kamimura M, Kinoshita T, Itoh H, Yuzawa Y, Takahashi J, Ohtsuka K. Eosinophilic granuloma of the spine: early spontaneous disappearance of tumor detected on magnetic resonance imaging. Case report. *J Neurosurg* 2000; 93:312-6; PMID:11012067; <http://dx.doi.org/10.3171/spi.2000.93.2.0312>
55. Meraouna A, Cizeron-Clairac G, Panse RL, Bismuth J, Truffault F, Tallaksen C, Berrih-Aknin S. The chemokine CXCL13 is a key molecule in autoimmune myasthenia gravis. *Blood* 2006; 108:432-40; PMID:16543475; <http://dx.doi.org/10.1182/blood-2005-06-2383>